Avoided crossings in three coupled oscillators as a model system of acoustic bubbles

Masato Ida*
Center for Promotion of Computational Science and Engineering, Japan Atomic Energy Research Institute, 6-9-3 Higashi-Ueno, Taito-ku, Tokyo 110-0015, Japan
(Received 19 April 2005; published 26 September 2005)

The resonance frequencies and oscillation phases of three acoustically coupled bubbles are examined to show that avoided crossings can appear in a multibubble system. Via a simple coupled oscillator model, we show that if at least three bubbles exist, it is possible for their resonance frequencies as functions of the separation distances between the bubbles to experience an avoided crossing. Furthermore, by focusing our attention on the oscillation phases and based on analysis of the transition frequencies [M. Ida, Phys. Lett. A **297**, 210 (2002); J. Phys. Soc. Jpn. **71**, 1214 (2002)] of the coupled bubbles, we show that a distinct state exchange takes place between the bubbles at a point in the avoided crossing region, where a resonance frequency of the triple-bubble system crosses with a transition frequency not corresponding to the resonance frequencies.

DOI: 10.1103/PhysRevE.72.036306 PACS number(s): 47.55.Dz, 43.20.+g, 47.55.Bx

I. INTRODUCTION

Avoided crossings [1] have been observed theoretically and experimentally in a large variety of physical systems involving eigenvalues (e.g., natural frequencies, eigenenergies) [2–15], and they have attracted much attention even in recent years because of their rich physics and practical importance in, for example, mechanical engineering [11–14] and quantum physics [2–5]. In the avoided crossing regions, eigenvalues of the system first approach each other as a system parameter is varied but then veer abruptly from each other without crossing. In those regions a drastic change of some characteristic of the system occurs along the eigenvalue loci. In Ref. [12], for example, Pierre illustrated that the mode shapes of a disordered chain of coupled pendulums change in the regions where avoided crossings of the eigenfrequencies of the system take place. In that study, disorders in the lengths of the pendulums were used as the system parameters. Also, in Ref. [2], Walkup *et al.* studied in detail avoided crossings observed in the energy levels of diamagnetic hydrogen as functions of the magnetic field strength or the angular momentum, which lead to the diabatic exchange of the states of the wave functions. A study of Bose-Einstein condensation (BEC) [5] showed that in order to trap molecules created in an atomic BEC through a Feshbach resonance, an avoided crossing of two bound states of the molecules must be exploited, through which the vibrational quantum number and size of the trapped molecules change.

In the present paper, we show theoretically that avoided crossings can be observed in acoustically coupled bubbles, which has to the authors' knowledge not been stated in the literature. Furthermore, based on analyses of transition frequencies [16,17], we propose a way to detect a state exchange occurring in the avoided crossing region. The theoretical model used in this study, reviewed in Sec. II, is a forced coupled oscillator model that describes acoustic coupling of pulsating bubbles. Using the model, we show in Sec. III that if at least three bubbles exist, it is possible that the resonance frequencies of the bubbles exhibit an avoided crossing when they are plotted as functions of the separation distances between the bubbles. As has been demonstrated (e.g., Refs. [16,18]), in double-bubble systems, neither crossings nor avoided crossings of the resonance frequencies as functions of the separation distance are observed, since the higher of the two resonance frequencies of the systems increases and the lower one decreases as the bubbles approach each other. However, as shown in the present paper, by introducing one more bubble whose monopole (i.e., decoupled) resonance frequency crosses with one of the resonance frequencies of a double-bubble system, one can observe the avoided crossing of the resonance frequencies when all three bubbles are coupled.

In Sec. IV, we examine the phase properties of the three coupled bubbles to show that a state exchange actually occurred between the bubbles in the avoided crossing region. In this effort, the notion of a transition frequency plays an important role. The transition frequencies introduced in Refs. [16,17] are characteristic frequencies of acoustically coupled bubbles, around which the oscillation phase of bubbles inverts, e.g., from in phase to out of phase with the driving sound. It was proved in Ref. [17] that a bubble in an N-bubble system has up to $2N-1$ transition frequencies, only N ones of which correspond to the resonance frequencies of the system. That is, observing the transition frequencies allows us to obtain richer insight into the phase properties than that obtained by only observing the resonance frequencies. This notion has already been exploited as a powerful tool to understand the sign reversal of the secondary Bjerknes force [18,19] in which the oscillation phases play a crucial role. Using this notion and observing directly the oscillation phases, we show that the coupled bubbles exchange their oscillation states through the avoided crossing and state exchange takes place at the separation distances where an avoided crossing resonance frequency crosses with a transition frequency that is not a resonance frequency. The present findings appear to reveal a taste of bubbles' hidden complexity.

Section V summarizes this paper, and the Appendixes present additional remarks.

*Electronic address: ida@koma.jaeri.go.jp

II. COUPLED OSCILLATOR MODEL, RESONANCE FREQUENCY, AND TRANSITION FREQUENCY

The theoretical model used in the present study is a forced oscillator model in which N harmonic oscillators are coupled ([16,17] and references therein):

$$\ddot{e}_i + \omega_{i0}^2 e_i + \delta_i \dot{e}_i = -\frac{p_{\mathrm{ex}}}{\rho R_{i0}} - \frac{1}{R_{i0}} \sum_{j=1, j\neq i}^{N} \frac{R_{j0}^2}{D_{ij}} \ddot{e}_j$$

$$\text{for } i = 1,2,\ldots,N, \tag{1}$$

where N corresponds to the number of bubbles, R_{i0} is the equilibrium radius of bubble i, e_i is the deviation of radius assumed as $|e_i| \ll R_{i0}$, ω_{i0} is the monopole (angular) resonance frequency of bubble i, defined as

$$\omega_{i0} = \sqrt{\frac{3\kappa_i P_0 + (3\kappa_i - 1)2\sigma/R_{i0}}{\rho R_{i0}^2}}, \tag{2}$$

δ_i is the damping factor, the overdots denote the time derivation, p_{ex} is the pressure of the external sound, ρ is the density of the surrounding liquid, $D_{ij}(=D_{ji})$ is the separation distance between the centers of bubbles i and j, κ_i is the polytropic exponent of the gas inside the bubbles, P_0 is the static pressure, and σ is the surface tension. In this linear model, the following assumptions are made: the surrounding liquid is incompressible, the sound amplitude is sufficiently low, the separation distances are much larger than the bubbles' radii, and the shape deformation of the bubbles is negligible. The last term of Eq. (1), representing the pressures of the sounds that the neighboring bubbles emit, describes the acoustic coupling between the bubbles. As in the double-bubble case [20], this model may be assumed to be of third order with respect to the inverse of the separation distances (i.e., the truncated terms are of fourth or higher order); see Appendix A.

Using this model with $N=3$, a matrix equation for determining the amplitudes and phases of the radial oscillations is derived. Assuming $p_{\mathrm{ex}} = -P_a \exp(\mathrm{i}\omega t)$ and $e_i = \beta_i \exp(\mathrm{i}\omega t)$ with P_a being a positive constant, ω being the driving (angular) frequency, and β_i being a complex amplitude, we have

$$\mathbf{A}\begin{pmatrix}\beta_1\\ \beta_2\\ \beta_3\end{pmatrix} = -\frac{P_a}{\rho}\mathbf{I}, \tag{3}$$

where $\mathbf{A}$ is a 3×3 matrix whose elements $a_{i,j}(i,j=1,2,3)$ are defined as

$$a_{i,j} \equiv \begin{cases} R_{i0}[(X-\omega_{i0}^2) - \mathrm{i}\omega\delta_i] & \text{for } i=j, \\ \dfrac{R_{j0}^2}{D_{ij}}X & \text{otherwise,} \end{cases} \tag{4}$$

with

$$X \equiv \omega^2 \tag{5}$$

and $\mathbf{I} = (1,1,1)^T$. We should note here that essentially the same matrix equations can be found in previous papers (e.g., [17,21,22]). The solution of Eq. (3) is represented as

$$\begin{pmatrix}\beta_1\\ \beta_2\\ \beta_3\end{pmatrix} = -\frac{P_a}{\rho}\mathbf{A}^{-1}\mathbf{I} = -\frac{P_a}{\rho}\frac{|\mathbf{A}|^*\mathbf{C}\mathbf{I}}{|\mathbf{A}|^*|\mathbf{A}|}, \tag{6}$$

where $|\mathbf{A}|$ and $\mathbf{C}$ are the determinant and the cofactor matrix of $\mathbf{A}$, respectively, and $|\mathbf{A}|^*$ is the complex conjugate of $|\mathbf{A}|$. We used here an expression in which the denominator is real.

The eigenfrequencies of the system are determined by

$$|\mathbf{A}| = 0, \tag{7}$$

which is a cubic equation in terms of X. For $\delta_i \approx 0$, the roots of this equation are equivalent to the resonance frequencies of the system. The transition frequencies of bubble i, defined as the driving frequencies at which the phase difference between bubble i and the driving sound is $\pi/2$ (or $3\pi/2$) [16–18], are determined by

$$\mathrm{Re}(\tau_i) = 0, \tag{8}$$

where

$$\begin{pmatrix}\tau_1\\ \tau_2\\ \tau_3\end{pmatrix} \equiv |\mathbf{A}|^*\mathbf{C}\mathbf{I}. \tag{9}$$

(See Appendix B for the concrete forms of $|\mathbf{A}|$ and $\mathbf{CI}$.) From the mathematical proof given in Ref. [17], one knows that Eq. (8) is a fifth-order polynomial in terms of X, meaning that the bubbles may have up to five transition frequencies.

The phase delay of bubble i, denoted by ϕ_i, measured from the phase of the driving sound is determined using the atan2(y,x) function in the C language, which returns $\tan^{-1}(y/x) \in [-\pi, \pi]$, as

$$\phi_i = \begin{cases} \psi_i & \text{if } \psi_i \geqslant 0, \\ \psi_i + 2\pi & \text{otherwise,} \end{cases}$$

with

$$\psi_i = \mathrm{atan2}(-\mathrm{Im}(\tau_i), \mathrm{Re}(\tau_i)).$$

The next section shows that in certain cases an avoided crossing is observed in the solution of Eq. (7). In the discussion, to obtain real eigenfrequencies that correspond to the resonance frequencies of the triple-bubble system for weak damping, we for the moment assume $\delta_i \approx 0$ (but $\delta_i \neq 0$). Under this assumption, one obtains

$$\mathrm{Im}(|\mathbf{A}|) \approx \mathbf{0}, \tag{10}$$

$$|\mathbf{A}| \approx |\mathbf{A}|^*, \tag{11}$$

and

$$\tau_i \approx \mathrm{Re}(\tau_i). \tag{12}$$

The influences of the damping effect on the phase properties are briefly discussed in Sec. IV.

III. AVOIDED CROSSINGS OF RESONANCE FREQUENCIES

To begin with, a double-bubble system is briefly reconsidered to confirm that no avoided crossings are observed in the

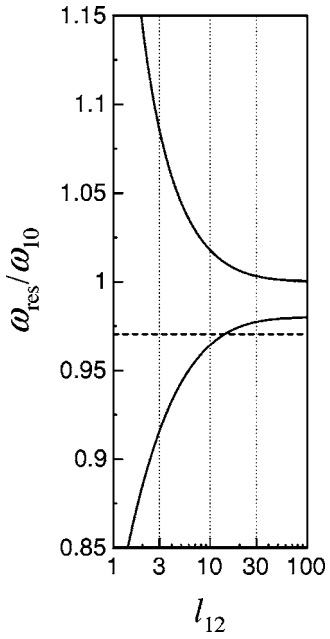

FIG. 1. Resonance frequencies ω_{res} (rad/s) of two coupled bubbles for $\delta_i \approx 0$ normalized by ω_{10} (rad/s), as functions of the normalized separation distance l_{12}. The dashed line denotes the monopole resonance frequency of a bubble that will be coupled with the former two bubbles in the next example.

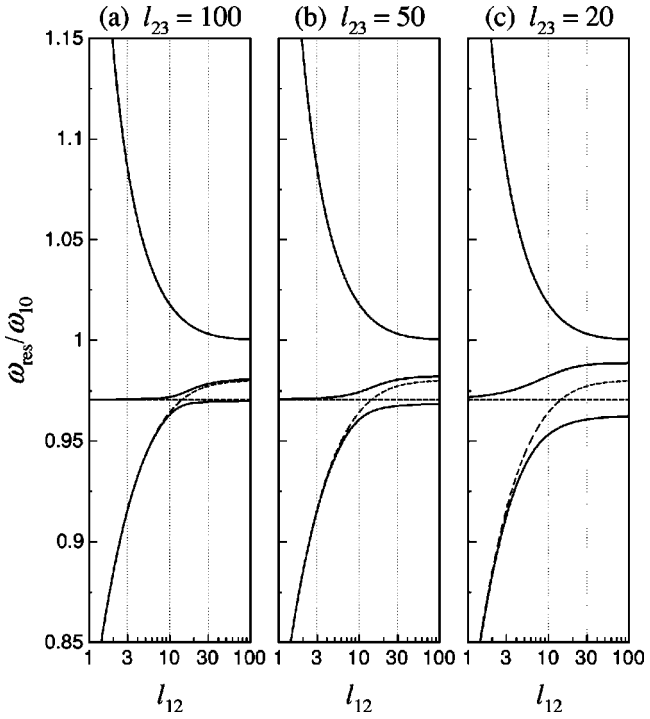

FIG. 2. Resonance frequencies ω_{res} (rad/s) of three coupled bubbles for $\delta_i \approx 0$ normalized by ω_{10} (rad/s), as functions of the normalized separation distance l_{12}. (a), (b), and (c) are for $l_{23}=100$, 50, and 20, respectively. The dashed lines denote the resonance frequencies when bubble 3 is decoupled.

resonance frequencies of the system as functions of the separation distance. The solid lines in Fig. 1 indicate the resonance frequencies of two coupled bubbles (bubbles 1 and 2) of $(R_{10},R_{20})=(50\ \mu\text{m},51\ \mu\text{m})$ as functions of $l_{12}=D_{12}/(R_{10}+R_{20})$. The other parameters are set to $\rho=1000\ \text{kg/m}^3$, $\kappa_i=1.4 (i=1,2,3)$, $P_0=1$ atm, and $\sigma=0.0728\ \text{N/m}$. As has been proved theoretically [16,20,23,24], two resonance (or natural) frequencies appear in this system, each of which, for $D_{12}\to\infty$, converges to the monopole resonance frequency of a bubble. The higher resonance frequency increases and the lower decreases as the separation distance decreases. It is therefore obvious that avoided crossings cannot occur.

Here we introduce one more bubble into the system. The dashed line displayed in Fig. 1 denotes the monopole resonance frequency of the introduced bubble, bubble 3, whose radius $R_{30}=51.5\ \mu\text{m}$. Note that this resonance frequency crosses with a resonance frequency of the double-bubble system. This crossing, as shown immediately, triggers an avoided crossing when the third bubble is coupled with the double-bubble system.

Figure 2 shows the resonance frequencies in the case where all three bubbles are coupled. The separation distances are set to $D_{12}=l_{12}(R_{10}+R_{20})$, $D_{23}=l_{23}(R_{20}+R_{30})$, and $D_{31}=D_{12}+D_{23}$; that is, the bubbles are arranged in line [see Fig. 3(a)]. Here the nondimensional quantities l_{12} and l_{23} are used as the system parameters. Figures 2(a)–2(c) show the results for $l_{23}=100$ [25], 50, and 20, respectively. In the figures, an avoided crossing is clearly seen that takes place around the point at which the two decoupled resonance frequencies cross. The line of the resonance frequency originating with bubble 3 is divided into two parts, and each of them connects smoothly, like blending, with the curve of a resonance frequency of the double-bubble system, also divided into two parts. As bubble 3 comes closer to the others, the avoided crossing becomes broader and the origin of each resonance frequency becomes increasingly unclear.

An avoided crossing is also observed when bubble 3 is smaller than the others. Figure 4 shows the resonance frequencies when $R_{30}=49.5\ \mu\text{m}$. Here the bubbles are arranged as illustrated in Fig. 3(b). If bubble 3 is so large or so small that its monopole resonance frequency does not cross with a resonance frequency of the double-bubble system, no distinct

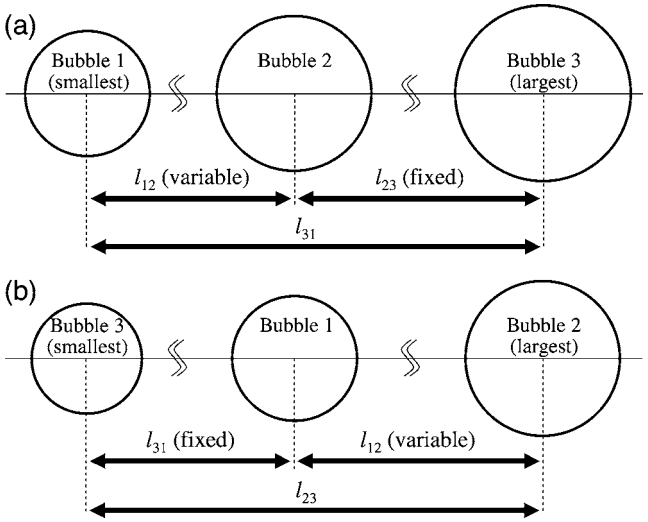

FIG. 3. Arrangements of bubbles in the cases where bubble 3 is larger (a) and smaller (b) than the other two bubbles.

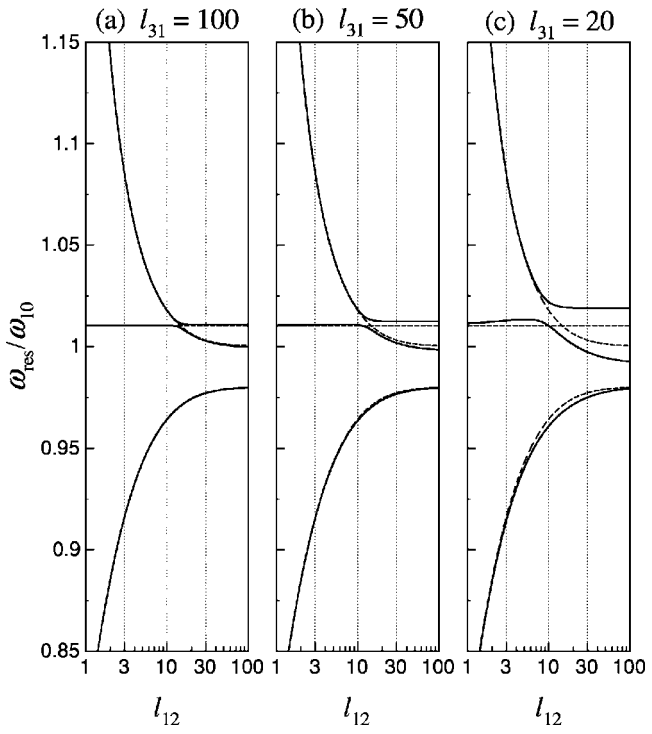

FIG. 4. Same as Fig. 2, but bubble 3 is smaller than the others. The bubbles are aligned as shown in Fig. 3(b).

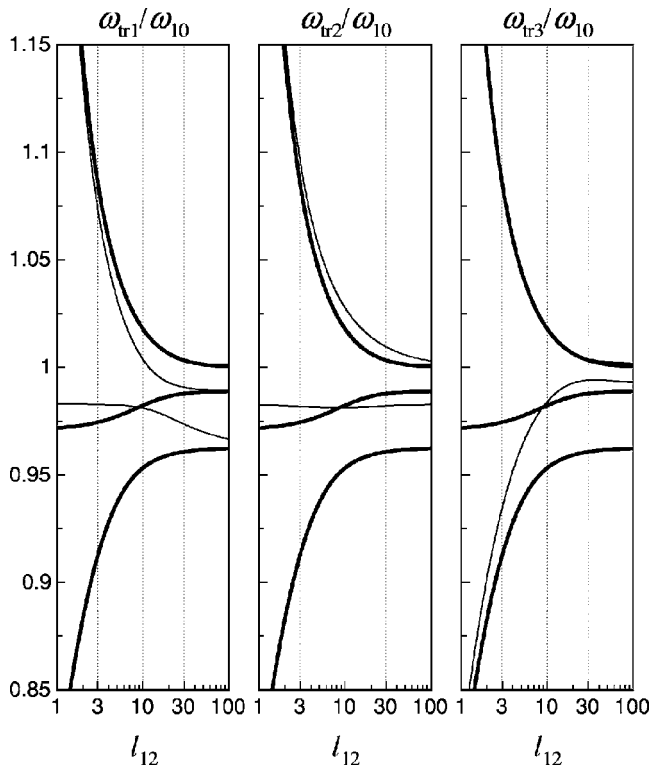

FIG. 5. Transition frequencies ω_{tr} (rad/s) of three coupled bubbles for $\delta_i \approx 0$ with $l_{23}=20$ normalized by ω_{10} (rad/s), as functions of the normalized separation distance l_{12}. ω_{tri} denotes the transition frequencies of bubble i.

avoided crossing is observed, though this situation is not shown here.

IV. STATE EXCHANGE IN THE AVOIDED CROSSING REGION

To manifest a state exchange like that which the coupled bubbles experience through the avoided crossing, we examined the oscillation phases of the bubbles. In bubble dynamics, the phase of radial oscillation plays important roles in many situations, including acoustic levitation [26–28], bubble-bubble interaction [18], and multibubble sonoluminescence [29], and hence an accurate understanding of it is crucial. In fact, by carefully examining the oscillation phases of two coupled bubbles for weak driving, we have recently succeeded in presenting a novel interpretation, which may be more accurate than previous ones, of the sign reversal of the secondary Bjerknes force [18,19], a paradoxical phenomenon that is considered to be the cause of the stable structure formation of bubbles in a weak acoustic field [24,30]. In that discussion, it was suggested that the transition frequencies seem to be essential components for gaining an accurate understanding of the phenomenon, since the sign reversal takes place at the transition frequencies that cannot be obtained by resonance-frequency analysis. In the present paper, we show by examining the oscillation phases that the bubbles exchange their oscillation states through the avoided crossing. As shown later, the point at which the state exchange occurs can be clearly detected by observing the transition frequencies.

Figure 5 shows the transition frequencies for $(R_{10},R_{20},R_{30})=(50\ \mu\text{m},51\ \mu\text{m},51.5\ \mu\text{m})$ with $l_{23}=20$. The thick lines denote the transition frequencies that correspond to the resonance frequencies already shown in Fig. 2(c). As expected from the mathematical proof presented in [17], the bubbles have up to five transition frequencies, all of which invert the oscillation phase of the corresponding bubble. It is worth noting that in each panel of Fig. 5 the second-highest resonance frequency (denoted below by ω_{2nd}) crosses once with a transition frequency in the avoided crossing region. Such crossings have not been found in double-bubble systems [16,18]. In the following discussion, we focus our attention on the phase properties of the bubbles in this region to elucidate what happens around the intersecting points.

The phase delays ϕ_i for different l_{12} as functions of ω/ω_{10} are shown by the solid lines in Fig. 6. In the computation of ϕ_i, we used very small but nonzero δ_i to obtain continuous results. Figures 6(a,b) and 6(c,d), respectively, show ϕ_i for l_{12} smaller and larger than the intersecting point $l_{12}=l_{int}(\approx 8.89)$. Here, we only displayed ϕ_i in the frequency range around the two avoided crossing resonance frequencies. The vertical dotted lines indicate the two lowest resonance frequencies. As in double-bubble cases [18,19], at the resonance frequencies the phase delays of all bubbles shift simultaneously by $+\pi$, whereas at the remaining transition frequencies only one phase delay shifts by $-\pi$.

The ϕ_i curves, as can be clearly seen in the figures, have different convexities on different sides of the intersecting point. For l_{12} smaller than l_{int}, at ω_{2nd}, ϕ_1 and ϕ_2 shift from π to 2π but ϕ_3 shifts from 0 to π as ω increases. For l_{12} larger than l_{int}, on the other hand, an opposite tendency is

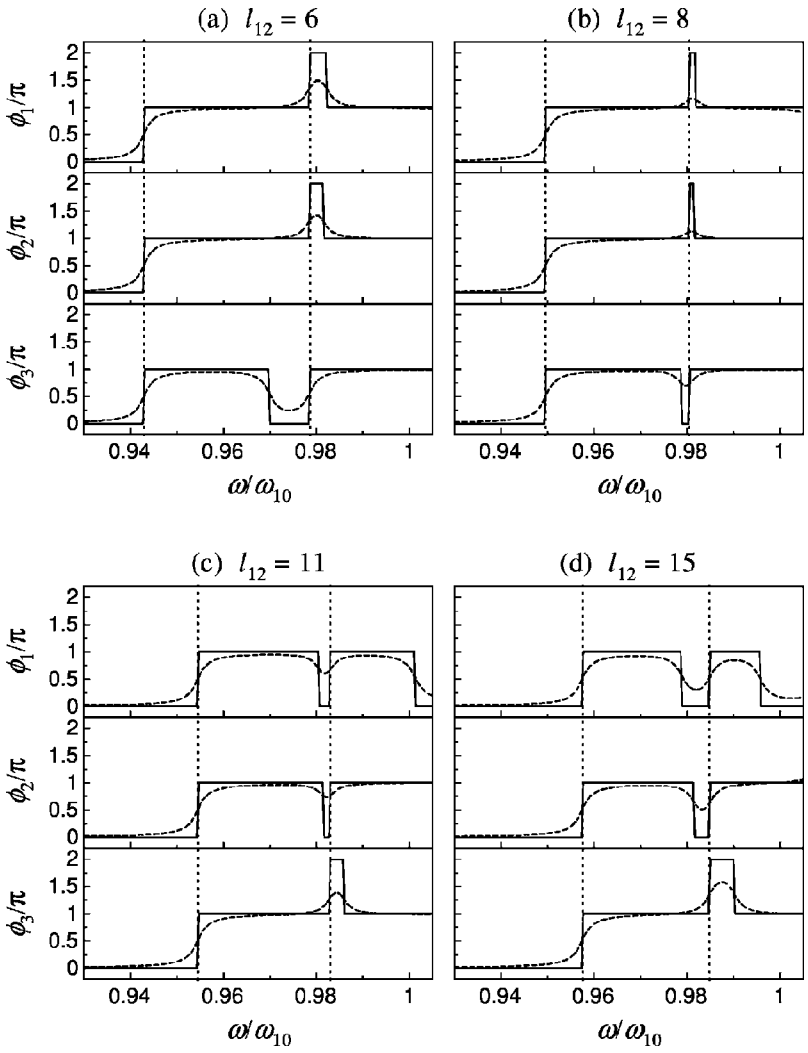

FIG. 6. Phase delays ϕ_i (rad) normalized by π as functions of ω/ω_{10} for different l_{12} [(a), (b) for $l_{12}<l_{\text{int}}$, (c), (d) for $l_{12}>l_{\text{int}}$]. The solid and the dashed curves denote ϕ_i for negligible and non-negligible damping, respectively, and the vertical dotted lines indicate the two lowest resonance frequencies (the higher is thus the second-highest resonance frequency $\omega_{2\text{nd}}$).

seen: ϕ_1 and ϕ_2 shift from 0 to π but ϕ_3 shifts from π to 2π. That is, a kind of state exchange takes place between bubble 3 and the other two bubbles at the intersecting point.

Regarding the relationship between the state exchange and the phase properties, in the frequency range around $\omega_{2\text{nd}}$, bubble 3 oscillates out of phase with the other bubbles regardless of whether $l_{12}<l_{\text{int}}$ or $l_{12}>l_{\text{int}}$, although the individual phase delays experience rapid shifts at $\omega_{2\text{nd}}$. This means that the state exchange cannot be perceived accurately by observing whether the bubbles oscillate in phase or out of phase with each other or by observing the sign of the secondary Bjerknes force, which is determined by the cosine of the phase difference between two bubbles [31,32]. Just the individual phase delays (or transition frequencies) should be examined.

In the ϕ_i curves, we can find several similarities with double-bubble cases. Bubbles 1 and 2, or bubble 3, have a phase delay greater than π in the frequency range from $\omega_{2\text{nd}}$ to a certain higher frequency (equal to the next-higher transition frequency of the corresponding bubble). A similar observation can be found for double-bubble systems [18,19]. In Ref. [18] we discovered and elucidated that such a large phase delay can appear when two bubbles interact with each other through sound. In the double-bubble case, the larger one of the two bubbles has a phase delay greater than π in the frequency range between the higher of two resonance frequencies and the highest of the transition frequencies of the bubble. We can, for a wider frequency range, also find a similarity between the double- and triple-bubble cases. In the frequency range $\omega/\omega_{10}<0.995$, the profiles of ϕ_1 and ϕ_2 for $l_{12}<l_{\text{int}}$ and that of ϕ_3 for $l_{12}>l_{\text{int}}$ are very similar to the profile of the phase delay of the larger bubble in a double-bubble system; those phase delays first exhibit two sharp rises and then one sharp fall as ω increases. Also, the profiles of the remaining phase delays are very similar to that of the phase delay of the smaller bubble in a double-bubble system, exhibiting one sharp rise, one sharp fall, and then one sharp rise. This seems to indicate that in the frequency range considered, for $l_{12}<l_{\text{int}}$ bubbles 1 and 2 act as "larger bubbles" while bubble 3 acts as a "smaller bubble," but for $l_{12}>l_{\text{int}}$ each bubble acts in the opposite way; that is, the physical roles that the bubbles play are exchanged through the avoided crossing. This observation could also be interpreted as a result of the change of a physical meaning of $\omega_{2\text{nd}}$. As illustrated in Fig. 2, $\omega_{2\text{nd}}$ is a hybrid of two resonance frequencies having different origins. We assume here that the origin, or the principal origin, of each avoided crossing resonance frequency is switched at l_{int}. This assumption allows

us to consider that ω_{2nd} for $l_{12}<l_{int}$, for example, is the resonance frequency whose principal origin is bubble 3. This suggestion is consistent, not only with the observation for large l_{23} where the origin of each resonance frequency is relatively clear, but also with the above speculation that bubbles 3 acts as a "smaller bubble" for $l_{12}<l_{int}$, because ω_{2nd} is higher than the lowest resonance frequency that is one of the two avoided crossing resonance frequencies. The observation for $l_{12}>l_{int}$ can be interpreted in a similar manner.

Last, we briefly examine how the damping affects the state exchange. For the damping coefficient, we use the value for viscous damping,

$$\delta_i = \frac{4\mu}{\rho R_{i0}^2}, \tag{13}$$

with viscosity $\mu=1.002\times10^{-3}$ kg/(m s). The dashed curves in Fig. 6 show the phase delays in the damped case. The viscous effect smoothes the phase profiles, but the convexity of the curves is not altered from that for $\delta_i\approx0$, as in the double-bubble cases [18,19]. The state exchange is clearly detected even in the present case. The qualitative tendencies of the phase delays are not changed by the viscous damping.

V. CONCLUSION

We have shown theoretically that avoided crossings can be observed in the resonance frequencies of acoustically coupled gas bubbles plotted as functions of the separation distances. A state exchange taking place between the bubbles in the avoided crossing region has been clearly exhibited by examining the oscillation phases and transition frequencies of the coupled bubbles. We have clarified that the state exchange is perceived by observing the individual oscillation phases of the bubbles, not by observing whether the bubbles oscillate in phase or out of phase with each other. Since the individual phase (or more properly, the phase difference between a bubble and the external sound) determines the sign of the primarily Bjerknes force [26–28] acting on the corresponding bubble, this state exchange should play a role in, e.g., acoustic levitation using the force. The results of this study suggest that the transition frequencies introduced in Ref. [16] can be a useful tool for detecting the state exchange, which takes place at the separation distance where an avoided crossing resonance frequency crosses with a transition frequency that is not a resonance frequency. Though we only considered triple-bubble systems in a linear arrangement, extensions to systems containing a larger number of bubbles and in different arrangements may be straightforward. Also, nonlinear effects on the avoided crossings and oscillation phases could be examined using nonlinear models [20,21,29,33]. As with other physical systems, the avoided crossings in acoustically coupled bubbles might be real.

ACKNOWLEDGMENTS

The author thanks Dr. Akemi Nishida for valuable comments. This work was supported by a Grant-in-Aid for Young Scientists (B) (No. 17760151) from the Ministry of Education, Culture, Sports, Science, and Technology of Japan.

APPENDIX A

High-order nonlinear models for N pulsating bubbles in a liquid have been proposed, in which terms proportional to $D_{ij}^{-k}(k\geqslant2)$ appear that involve the translational velocities of the bubbles [21,33]. In Ref. [33], for example, Doinikov derived the following model equation for N spherical bubbles:

$$R_i\ddot{R}_i+\frac{3}{2}\dot{R}_i^2-\frac{P_i}{\rho}=\frac{\dot{\mathbf{p}}_i^2}{4}-\sum_{j=1,j\neq i}^{N}\left\{\frac{R_j^2\ddot{R}_j+2R_j\dot{R}_j^2}{D_{ij}}+H_{ij}\right\}, \tag{A1}$$

$$\frac{1}{3}R_i\ddot{\mathbf{p}}_i+\dot{R}_i\dot{\mathbf{p}}_i=\frac{\mathbf{F}_i}{2\pi\rho R_i^2}+\sum_{j=1,j\neq i}^{N}\left\{-\frac{1}{D_{ij}^2}(R_iR_j^2\ddot{R}_j+2R_iR_j\dot{R}_j^2+\dot{R}_i\dot{R}_jR_j^2)\mathbf{t}_{ij}-\frac{R_j^2}{2D_{ij}^3}[R_iR_j\ddot{\mathbf{p}}_j+(\dot{R}_iR_j+5R_i\dot{R}_j)\dot{\mathbf{p}}_j]+\frac{3R_j^2}{2D_{ij}^3}\{\mathbf{t}_{ij}\cdot[R_iR_j\ddot{\mathbf{p}}_j+(\dot{R}_iR_j+5R_i\dot{R}_j)\dot{\mathbf{p}}_j]\}\mathbf{t}_{ij}\right\}, \tag{A2}$$

with

$$H_{ij}\equiv-\frac{R_j^2}{2D_{ij}^2}(R_j\ddot{\mathbf{p}}_j+\dot{R}_j\dot{\mathbf{p}}_i+5\dot{R}_j\dot{\mathbf{p}}_j)\cdot\mathbf{t}_{ij}-\frac{R_j^3}{4D_{ij}^3}\{\dot{\mathbf{p}}_j\cdot(\dot{\mathbf{p}}_i+2\dot{\mathbf{p}}_j)-3(\dot{\mathbf{p}}_j\cdot\mathbf{t}_{ij})[\mathbf{t}_{ij}\cdot(\dot{\mathbf{p}}_i+2\dot{\mathbf{p}}_j)]\}, \tag{A3}$$

$$\mathbf{t}_{ij}\equiv\frac{\mathbf{p}_j-\mathbf{p}_i}{D_{ij}},$$

$$P_i\equiv\left(P_0+\frac{2\sigma}{R_{i0}}\right)\left(\frac{R_{i0}}{R_i}\right)^{3\gamma}-\frac{2\sigma}{R_i}-\frac{4\mu\dot{R}_i}{R_i}-P_0-p_{ex}, \tag{A4}$$

where R_i and $\mathbf{p}_i$ are the instantaneous radius and position vector, respectively, of bubble i, $\mathbf{F}_i$ denotes external forces on bubble i, $\mathbf{t}_{ij}$ is a unit vector, γ is the specific heat ratio of the gas inside the bubbles, and μ is the viscosity. Here we showed only the incompressible version, though Doinikov also derived a model for bubbles in a compressible liquid. Equations (A1) and (A2) represent the volume oscillation of bubble i and its translational motion, respectively. The linear coupled oscillator model used in the present study is recovered from Eq. (A1) by truncating the high-order terms H_{ij} and assuming weak driving and $\gamma=\kappa_i$.

Since the velocity field forming around a pulsating sphere is proportional to $1/r^2$, where r is the distance measured from the center of the sphere, the truncated terms H_{ij}, which are composed of the translational velocities $\dot{\mathbf{p}}_i$, might be considered to be of fourth, or higher, order with respect to the inverse of the separation distances. This speculation is consistent with the suggestion by Harkin *et al.* for double-bubble systems [20].

Equation (A1) further suggests that under the assumption of $\dot{\mathbf{p}}_i \approx \mathbf{0}$ one cannot construct a linear model that has higher-order accuracy than that of Eq. (1), since this assumption makes the high-order terms inaccurate.

APPENDIX B

For the convenience of readers, we show the concrete forms of $|\mathbf{A}|$ and $\mathbf{CI}$:

$$\begin{aligned}\frac{|\mathbf{A}|}{R_{10}R_{20}R_{30}} &= L_1L_2L_3 + s_{21}s_{32}s_{13} + s_{12}s_{23}s_{31} \\ &\quad - L_1(M_2M_3 + s_{23}s_{32}) - L_2(M_3M_1 + s_{31}s_{13}) \\ &\quad - L_3(M_1M_2 + s_{12}s_{21}) + \mathrm{i}[M_1M_2M_3 \\ &\quad - M_1(L_2L_3 - s_{23}s_{32}) - M_2(L_3L_1 - s_{31}s_{13}) \\ &\quad - M_3(L_1L_2 - s_{12}s_{21})], \end{aligned} \tag{B1}$$

$$\mathbf{CI} = (c_1, c_2, c_3)^T,$$

$$\begin{aligned}\frac{c_i}{R_{j0}R_{k0}} &= (L_j - s_{ij})(L_k - s_{ik}) + (s_{ij} - s_{kj})(s_{jk} - s_{ik}) - M_jM_k \\ &\quad + \mathrm{i}[M_j(s_{ik} - L_k) + M_k(s_{ij} - L_j)] \\ &\quad \text{for } (i,j,k) = (1,2,3),\ (2,3,1),\ \text{or } (3,1,2), \end{aligned} \tag{B2}$$

where

$$L_i \equiv X - \omega_{i0}^2,$$

$$M_i \equiv \omega\delta_i,$$

$$s_{ij} \equiv \frac{R_{j0}}{D_{ij}}X.$$

For $\delta_i \approx 0$, Eqs. (B1) and (B2) reduce, respectively, to

$$\begin{aligned}\frac{|\mathbf{A}|}{R_{10}R_{20}R_{30}} &\approx L_1L_2L_3 + s_{21}s_{32}s_{13} + s_{12}s_{23}s_{31} - L_1s_{23}s_{32} \\ &\quad - L_2s_{31}s_{13} - L_3s_{12}s_{21}, \end{aligned} \tag{B3}$$

$$\frac{c_i}{R_{j0}R_{k0}} \approx (L_j - s_{ij})(L_k - s_{ik}) + (s_{ij} - s_{kj})(s_{jk} - s_{ik}). \tag{B4}$$

Equation (B3) and the real part of Eq. (B1) are cubic functions, and Eq. (B4) and the real part of Eq. (B2) are quadratic functions in terms of X. The imaginary parts of Eqs. (B1) and (B2) can be written in a form of $\omega f(X)$, where f is quadratic in Eq. (B1) and linear in Eq. (B2). (As proved theoretically in Ref. [17], the imaginary parts are composed of terms of odd orders with respect to M which are proportional to ωX^n with n being a positive integer.)

[1] In the fields of vibration engineering and some others, avoided crossings are called "curve veering," "eigenvalue veering," or "(natural) frequency loci veering." They are also sometimes called "avoided level crossings."
[2] J. R. Walkup, M. Dunn, D. K. Watson, and T. C. Germann, Phys. Rev. A **58**, 4668 (1998).
[3] T. Timberlake and L. E. Reichl, Phys. Rev. A **59**, 2886 (1999).
[4] S. Li and E. J. Heller, Phys. Rev. A **67**, 032712 (2003).
[5] S. Dürr, T. Volz, A. Marte, and G. Rempe, Phys. Rev. Lett. **92**, 020406 (2004).
[6] Y. Osaki, Publ. Astron. Soc. Jpn. **27**, 237 (1975).
[7] D. Gondek and J. L. Zdunik, Astron. Astrophys. **344**, 117 (1999).
[8] S. Shaik, A. Ioffe, A. C. Reddy, and A. Pross, J. Am. Chem. Soc. **116**, 262 (1994).
[9] C. Zhu and H. Nakamura, Chem. Phys. Lett. **274**, 205 (1997).
[10] J. R. Kuttler and V. G. Sigillito, J. Sound Vib. **75**, 585 (1981).
[11] N. C. Perkins and C. D. Mote Jr., J. Sound Vib. **106**, 451 (1986).
[12] C. Pierre, J. Sound Vib. **126**, 485 (1988).
[13] H. H. Yoo and S. H. Shin, J. Sound Vib. **212**, 807 (1998).
[14] R. S. Langley, Proc. R. Soc. London, Ser. A **455**, 3325 (1999).
[15] A. A. Mailybaev, O. N. Kirillov, and A. P. Seyranian, J. Phys. A **38**, 1723 (2005).
[16] M. Ida, Phys. Lett. A **297**, 210 (2002).
[17] M. Ida, J. Phys. Soc. Jpn. **71**, 1214 (2002).
[18] M. Ida, Phys. Rev. E **67**, 056617 (2003).
[19] M. Ida, J. Phys. Soc. Jpn. **73**, 3026 (2004).
[20] A. Harkin, T. J. Kaper, and A. Nadim, J. Fluid Mech. **445**, 377 (2001).
[21] H. Takahira, T. Akamatsu, and S. Fujikawa, JSME Int. J., Ser. B **37**, 297 (1994).
[22] C. Feuillade, J. Acoust. Soc. Am. **98**, 1178 (1995).
[23] A. Shima, Trans. ASME, J. Basic Eng. **93**, 426 (1971).
[24] E. A. Zabolotskaya, Sov. Phys. Acoust. **30**, 365 (1984).
[25] For such a large separation distance, in practice the time delay effect due to the finite sound speed of the surrounding liquid should be taken into account, though we only present an idealized result for the sake of simplicity.
[26] F. G. Blake Jr., J. Acoust. Soc. Am. **21**, 551 (1949).
[27] T. J. Matula, Philos. Trans. R. Soc. London, Ser. A **357**, 225 (1999).
[28] I. Akhatov, R. Mettin, C. D. Ohl, U. Parlitz, and W. Lauterborn, Phys. Rev. E **55**, 3747 (1997).
[29] R. Mettin, I. Akhatov, U. Parlitz, C. D. Ohl, and W. Lauterborn, Phys. Rev. E **56**, 2924 (1997).
[30] A. A. Doinikov and S. T. Zavtrak, J. Acoust. Soc. Am. **99**, 3849 (1996).
[31] W. Lauterborn, T. Kurz, R. Mettin, and C. D. Ohl, Adv. Chem. Phys. **110**, 295 (1999).
[32] L. A. Crum, J. Acoust. Soc. Am. **57**, 1363 (1975).
[33] A. A. Doinikov, J. Acoust. Soc. Am. **116**, 821 (2004).